

## The Influence of the Morphology on the Dynamics in Ordered Diblock Copolymer Melts

Christine M. Papadakis,<sup>1,2,\*</sup> Kristoffer Almdal,<sup>2</sup> Kell Mortensen,<sup>2</sup>

Frank Rittig,<sup>1,§</sup> and Petr Štěpánek<sup>3</sup>

<sup>1</sup>Fakultät für Physik und Geowissenschaften, Universität Leipzig, Linnéstr. 5, D-04103 Leipzig, Germany

<sup>2</sup>Condensed Matter Physics and Chemistry Department, Risø National Laboratory, P.O. Box 49, DK-4000 Roskilde, Denmark

<sup>3</sup>Institute of Macromolecular Chemistry, Academy of Sciences of the Czech Republic, Prague, Czech Republic

Dedicated to Gerald Fleischer who deceased June 16, 1999.

**SUMMARY:** We report on polarized and depolarized dynamic light scattering (DLS) measurements on two asymmetric poly(ethylene-*alt*-propylene-*block*-dimethylsiloxane) (PEP-PDMS) diblock copolymers in bulk. Apart from the disordered phase, the samples form various ordered morphologies below their respective order-to-disorder transition temperatures: One of the samples forms the hexagonal structure composed of PEP cylinders in a PDMS matrix, whereas the other one forms three ordered structures as a function of temperature, among them two cubic micellar structures and a non-cubic structure. We report here on the dynamic processes found in polarized DLS measurements in the disordered, hexagonal, cubic micellar and non-cubic structure in the same material.

### Introduction

Many soft materials, such as liquid crystals, surfactant and lipid solutions, are structured on a mesoscopic lengthscale. The interfaces formed in these self-assembled structures influence both the molecular dynamics, e.g. the diffusion of single molecules,<sup>1)</sup> as well as the collective dynamics.<sup>2)</sup> Diblock copolymers, which consist of two chemically distinct blocks, also form structured microphase-separated, ordered structures, such as micellar cubic, cylindric

---

<sup>§</sup> Present address: Air Products and Chemicals, 7201 Hamilton Blvd., Allentown, PA 18195, USA

hexagonal or lamellar phases and represent thus a model system for studying the influence of the morphology on the dynamics. The origin of the formation of microphase-separated, ordered structures is the generally repulsive interaction between the two types of segments, described by the Flory-Huggins segment-segment interaction parameter  $\chi$ , which is inversely proportional to temperature.<sup>3)</sup> Microphase separation into ordered morphologies takes place for values of the combined parameter  $\chi N$  larger than  $(\chi N)_{\text{ODT}}$  ( $N$  is the overall degree of polymerization, and ODT stands for order-disorder transition). The structure formed depends on the volume fraction of one block,  $f$ . Below  $(\chi N)_{\text{ODT}}$  (which also depends on  $f$ ), a disordered melt is formed with concentration fluctuations on a length scale of the overall polymer radius of gyration. In the disordered state, the diffusion of block copolymers is isotropic. In the ordered morphologies, chain diffusion is expected to proceed more easily along the interfaces separating the two types of blocks than across. In the lamellar and the cylindrical morphology, this would lead to anisotropic diffusion along the interfaces. In the micellar state, on the other hand, the motion of chains along the interface would not correspond to long-range diffusion, and we expect completely different diffusion mechanisms in this phase. Diblock copolymers in the bulk (e.g. without solvent present) – which are the topic of the present contribution – differ from the above mentioned systems (lipid and surfactant systems) in that they form a single component dense melt and in that both blocks are amorphous, in contrast to liquid crystals.

Even in the isotropic disordered state, the dynamics of diblock copolymer systems in the bulk have proven to be complex.<sup>4)</sup> So far, mostly compositionally symmetric samples have been studied. In these samples in the disordered state, two dynamic processes have been both theoretically predicted and observed using dynamic light scattering (DLS): the heterogeneity mode, governed by self-diffusion of the chains<sup>5,6)</sup> and the internal mode, corresponding to the relative movement of the two blocks.<sup>6-8)</sup> The heterogeneity mode is characterized by a  $q^2$ -dependent relaxation rate  $\Gamma_{\text{H}} = D_{\text{H}} q^2$  (H stands for heterogeneity and  $q$  is the scattering vector). Here,  $D_{\text{H}}$  is given by<sup>5)</sup>

$$D_{\text{H}} = D_{\text{self}} (1 - 2\chi N(\delta f)^2) \quad (1)$$

where  $D_{\text{self}}$  is the diffusion coefficient of self-diffusion and  $\delta f$  describes the heterogeneity in composition and is for symmetric diblock copolymers defined by

$$(\delta f)^2 = \frac{\overline{M}_w - \overline{M}_n}{4\overline{M}_w} \quad (2)$$

It has been assumed that the polydispersities of the two blocks are statistically independent,  $\overline{M}_w$  and  $\overline{M}_n$  are the weight- and number-averages of molar mass. The amplitude of the heterogeneity mode is  $q$ -independent. The internal mode has a  $q$ -independent relaxation rate, but its amplitude  $S_I(q)$  has been predicted<sup>7)</sup> to increase with  $q^2$ :

$$S_I(q) \cong \frac{2}{3} N v f^2 (1-f)^2 (q R_g)^2 \quad (3)$$

where  $v$  is the segment volume and  $R_g$  the overall radius of gyration. As the amplitude of the internal mode for Gaussian chains ( $R_g \propto N^{1/2}$ ) is proportional to  $N^2$ , it is usually not observed for block copolymers having low molar masses. Near the ODT, two additional dynamic processes have been observed experimentally in symmetric diblock copolymers in the disordered state: a second  $q^2$ -dependent mode, termed X-mode, has been attributed to undulations of transient lamellar interfaces,<sup>9,10)</sup> and a  $q$ -independent mode giving rise to depolarized scattering as well, attributed to the rotation of stretched chains<sup>11-13)</sup> or to the reorientational dynamics of transient lamellar domains.<sup>10)</sup> Also, the segmental reorientational dynamics of the two types of segments have been observed (e.g. Ref. 13). Another mode frequently observed in the disordered state is slow and is often of high amplitude. It was tentatively assigned to the diffusion of clusters, i.e. long-range heterogeneities appearing in the vicinity of the glass transition.<sup>14)</sup> As this mode has been observed in other polymeric systems as well, it is probably not related to the inherent block copolymer dynamics.<sup>15)</sup> In the ordered state, an even slower and very broad mode of lower relative amplitude is observed instead, which may be attributed to the dynamics of ordered domains. In the ordered, lamellar state formed by symmetric diblock copolymers, non-entangled diblock copolymers were found to diffuse mainly along the interfaces, the diffusion across the interfaces being hindered by the repulsive interaction between different segments.<sup>16)</sup> This anisotropic diffusion was confirmed using pulsed field gradient (PFG) NMR on a symmetric PEP-PDMS sample.<sup>17)</sup> The X-mode mentioned above was not observed in the PFG NMR experiment, i.e. it is not a self-diffusive process.<sup>17)</sup>

Only recently, the dynamics of asymmetric diblock copolymers have been studied. Using DLS, Vogt et al. studied a polystyrene-poly(methylphenylsiloxane) sample in the hexagonal phase.<sup>18)</sup> They attributed the single diffusive mode observed to the translational diffusion of cylinders. Using forced Rayleigh scattering and PFG NMR, Hamersky et al. investigated an asymmetric poly(ethylene oxide-*block*-ethylene) sample forming, among others, the hexagonal phase.<sup>19)</sup> Two dynamic processes were observed in the hexagonal state: The faster

one was assigned to the diffusion of chains along and across the cylinder interfaces and the slower one to the diffusion of chains through imperfectly ordered regions.<sup>19)</sup>

The dynamics in the micellar state have been found to be qualitatively different from the lamellar and the hexagonal state: In computer simulations on an asymmetric diblock copolymer system forming a micellar ordered state, at short times, only subdiffusive behavior was found and long-range diffusion only at long times.<sup>20)</sup> The micelles were not found to move in the time window of the simulation.<sup>20)</sup> In a PFG NMR study of the self-diffusion in a strongly asymmetric poly(styrene-*block*-isoprene) diblock copolymer melt in the body-centered cubic structure, both the self-diffusion of free chains, i.e. chains not bound to micelles, and the self-diffusion of entire micelles were observed.<sup>21)</sup> In a forced Rayleigh scattering study on a shear oriented, asymmetric poly(ethylene propylene-*block*-ethylethylene) diblock copolymer sample showing an order-order transition (OOT) from the cylindrical to the spherical state,<sup>22)</sup> no discontinuity in the diffusion coefficient was found at the OOT. In both morphologies, the diffusion coefficients along and across the interfaces were found to be very similar, which was attributed to the entanglements hindering the diffusion along the interfaces.<sup>22)</sup> Using forward recoil spectroscopy, Yokoyama et al. found the self-diffusion of single chains in an ordered spherical poly(styrene-*block*-2-vinylpyridine) sample to be four orders of magnitude slower than the one of polystyrene homopolymer having the same molar mass.<sup>23)</sup> They attributed this fact to the thermodynamic barriers for chain diffusion from one micelle to another.<sup>23)</sup>

We have previously studied the relation between structure and dynamics of symmetric<sup>10,17)</sup> and asymmetric, cylinder-forming<sup>24)</sup> and micelle-forming poly(ethylene-*alt*-propylene-*block*-dimethylsiloxane) (PEP-PDMS) samples<sup>25-27)</sup> using small-angle neutron scattering (SANS),<sup>25)</sup> DLS,<sup>10,26)</sup> and PFG NMR.<sup>17,24,27,28)</sup> In the symmetric sample, DLS enabled us to identify the heterogeneity mode, undulations of the lamellar interfaces (the 'X-mode') similar to the ones found in other layered systems, such as lipid bilayers, and – in the depolarized geometry – the rotation of lamellar domains. Using PFG NMR, a broad distribution of diffusion coefficients was observed in the lamellar state, which we attributed to the orientational distribution of lamellar domains.<sup>17)</sup> The diffusion constant increases discontinuously upon heating through the ODT temperature with a narrower distribution of diffusion constants in the disordered state.<sup>17)</sup> The PFG NMR results of the hexagonal sample were interpreted in terms of a model for anisotropic diffusion along and across the cylinder interfaces,<sup>24)</sup> and the anisotropy of

diffusion (along and across the cylinder interfaces) was found to be a factor of 5 near the ODT to 60 deep in the hexagonal state. As both in the lamellar and the hexagonal sample the ordered domains were randomly distributed, the powder average was used in the data analyses. We have studied another sample which forms three ordered morphologies apart from the disordered state, among them a cubic morphology, a non-cubic morphology and the body-centered cubic morphology (decreasing temperature).<sup>25)</sup> The dynamics of this sample have been studied using DLS in the polarized geometry<sup>26)</sup> and PFG NMR,<sup>27,28)</sup> and the results from DLS will be reviewed here together with the findings on a sample forming the disordered and the hexagonal morphology. In both cases, the micelles and cylinders, respectively, consist of PEP, the minority phase.

## Experimental

### The Samples

Two poly(ethylene-*alt*-propylene-*block*-dimethylsiloxane) (PEP-PDMS) diblock copolymer samples were studied. Their characteristics are given in Table I. The samples were synthesized using standard anionic polymerization techniques<sup>29-31)</sup> with the PEP blocks being partly deuterated. The  $\chi$ -parameter of PEP-PDMS is 63 K/T-0.04.<sup>30)</sup> The glass transition temperatures of the corresponding homopolymers are -56 °C for PEP<sup>32)</sup> and -127 °C for PDMS.<sup>33)</sup>

Table I: Characteristics of the two diblock copolymers studied.

Sample	$\overline{M}_n$ (kg/mol)	N <sup>(a)</sup>	$\overline{M}_w / \overline{M}_n$ <sup>(b)</sup>	$f_{\text{PEP}}$ <sup>(c)</sup>	T <sub>ODT</sub> (°C) <sup>(d)</sup>	Repeat distance (nm) <sup>(e)</sup>
PEP-PDMS 21	13.0	211	1.11	0.25	187	25 - 27
PEP-PDMS 22	12.5	203	1.08	0.22	134	19 - 22

(a) Degree of polymerization based on a segment volume of 118 Å<sup>3</sup>,<sup>30)</sup> (b) determined using size-exclusion chromatography (SEC),<sup>30)</sup> (c) from stoichiometry and NMR,<sup>30)</sup> (d) from the DLS experiments (see text), (e) from SANS experiments<sup>25)</sup>.

### Transmitted Depolarized Light Intensity

It has been shown<sup>34)</sup> that polycrystalline samples are birefringent even when the individual grains are randomly oriented, provided each grain is birefringent itself. Here, measurements

of the transmitted depolarized light intensity were conducted as described in Ref. 25 and allowed the determination of the ODT and OOT temperatures.

### Dynamic Light Scattering

Dust-free samples for dynamic light scattering (DLS) measurements were prepared by dissolving the polymers in *n*-hexane and filtering the solutions into the previously dedusted scattering cells. The solvent was removed by heating the dried samples over the ODT temperature under vacuum, and the cells were sealed under vacuum. The DLS experiments were conducted using a Coherent Innova-70 Ar<sup>+</sup>-laser ( $\lambda = 514$  nm) as a light source and an ALV 5000/E correlator. Details on the setup can be found in Ref. 10. Measurements were conducted in the polarized (VV) geometry. The measured intensity correlation functions  $G_2(t)$  were analyzed by inverse Laplace transformation using the routine REPES.<sup>35)</sup> By means of a subtraction routine described in Refs. 13 and 36, single decays (peaks in the distribution function of relaxation times) can be subtracted from the correlation curve and the remainder be re-analyzed using REPES. It has been shown before<sup>36)</sup> and was verified for the present correlation curves that the subtraction does not influence the relaxation rates and amplitudes of the faster modes. From the distribution functions of relaxation times,  $\tau A(\tau)$  vs.  $\log(\tau)$ , the mean relaxation times of each mode were extracted as the centers of mass of the peaks.

## Results and Discussion

### The Disordered and the Hexagonal Morphology

The transmitted depolarized intensity of sample PEP-PDMS 21 (Table I) has a constant value below  $\sim 190$  °C and a much lower value above (Fig. 1a). We assign this discontinuous drop to the ODT from the hexagonal to the disordered state. Note that the exact value of  $T_{\text{ODT}}$  depends on the heating/cooling rate.

Typical time-dependent intensity autocorrelation functions in the polarized geometry,  $G_2^{\text{VV}}(t) - 1$ , in the disordered and the hexagonal state are shown in Fig. 2a. In the disordered state, the correlation functions are dominated by the so-called cluster mode. The diffusion constant of this mode increases from  $4.3 \times 10^{-15}$  m<sup>2</sup>/s at the ODT temperature to  $2.6 \times 10^{-14}$  m<sup>2</sup>/s at 236 °C, as determined from a fit of two stretched exponentials to the whole time range of the intensity autocorrelation function. The cluster mode is close to single-exponential, and its relative

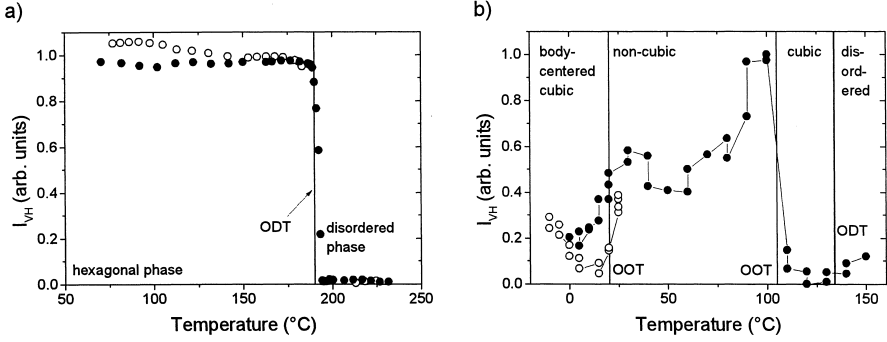


Fig. 1: Transmitted depolarized light intensity,  $I_{VH}$ , as a function of temperature. (o) Heat, (●) cool. The vertical lines indicate the ODT and OOT temperatures, respectively. (a) PEP-PDMS 21, heating and cooling rates smaller than 0.7 °C/min. (b) PEP-PDMS 22. The first data point at each temperature was measured after 1 hour and the second one after 10 h.

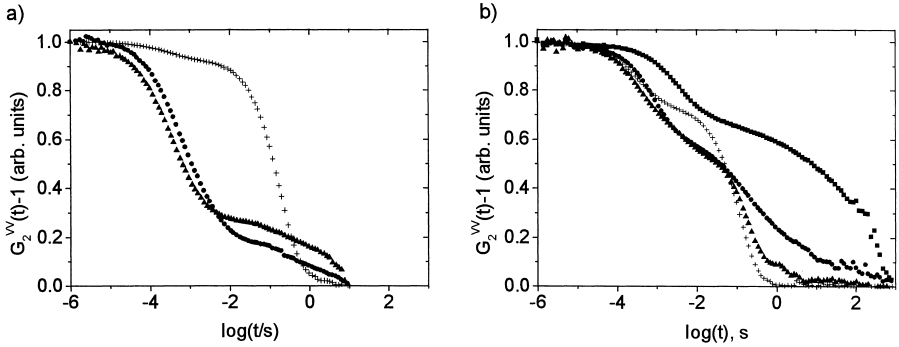


Fig. 2: Intensity autocorrelation functions from DLS at a scattering angle  $\theta = 90^\circ$ . For clarity, only every second data point is shown. (a) PEP-PDMS 21: (●) 137 °C, (▲) 177 °C, and (+) 197 °C. (b) PEP-PDMS 22: (■) 7 °C, (●) 62 °C, (▲) 125 °C, and (+) 167 °C.

amplitude is above 93 % throughout the whole temperature range in the disordered state. The origin of the cluster mode in block copolymer and other systems is still under discussion.<sup>37)</sup> The fact that the relative amplitude of the cluster mode does not decrease with increasing temperature is astonishing since the cluster mode often has been tentatively assigned to the proximity of the glass transition,<sup>38)</sup> and the measurements presented here have been made more than 240 °C (and up to ~300 °C) above the highest glass transition temperature of PEP-PDMS. In the hexagonal state, the slowest mode is very broad. As it is only partly present in the experimental time window, it has a relatively small amplitude in the ordered state.

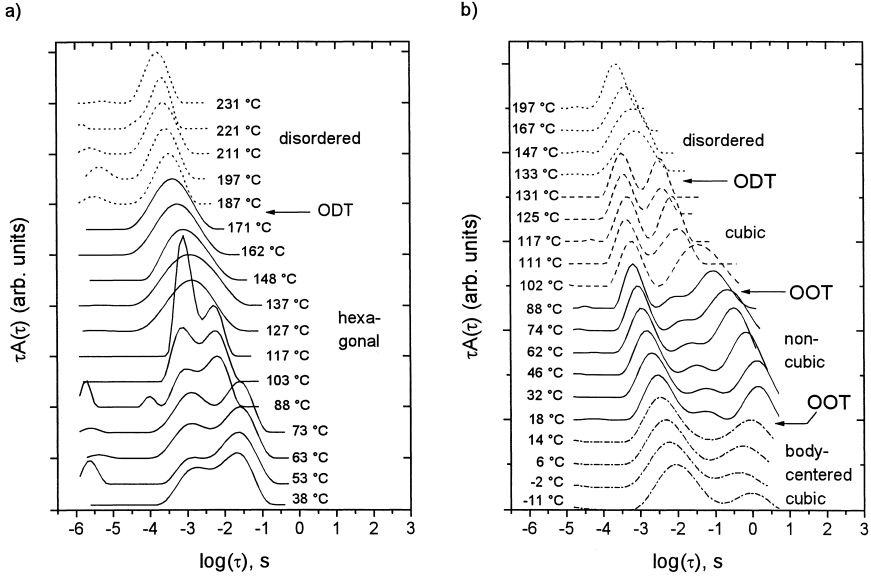


Fig. 3: Typical distribution functions of relaxation times from DLS at  $\theta = 90^\circ$  in the disordered and the hexagonal state, shifted by arbitrary amounts. (a) PEP-PDMS 21, the cluster mode has been subtracted at all temperatures. (b) PEP-PDMS 22, the cluster mode has been subtracted for  $T \geq 111^\circ\text{C}$ .

The slow modes, i.e. the cluster mode in the disordered state and the slow and broad mode in the hexagonal state discussed were subtracted from the correlation curves (see Exp. Section), and the remainders were analyzed using REPES. The resulting distribution functions are shown in Fig. 3a in the equal area format,  $\tau A(\tau)$  vs.  $\log(\tau)$ . In the disordered state, a mode is observed which persists throughout the ODT and splits up into two modes at  $\sim 127^\circ\text{C}$ . Below this temperature, the relative amplitude (i.e. the area under the peak) of the fast mode with respect to the slower mode increases with temperature. For all modes observed, the relaxation rate  $\Gamma$  is proportional to  $q^2$  (Fig. 4), i.e. diffusive with a diffusion coefficient that can be calculated from the mean relaxation times  $\tau$  using  $D = (\tau q^2)^{-1}$ . The determined diffusion coefficients of all modes except the cluster mode are compiled in an Arrhenius-diagram (Fig. 5a). In order to assign the modes to dynamic processes, the diffusion coefficients of PEP and PDMS homopolymers (scaled to the overall block copolymer molar mass) are given as well,

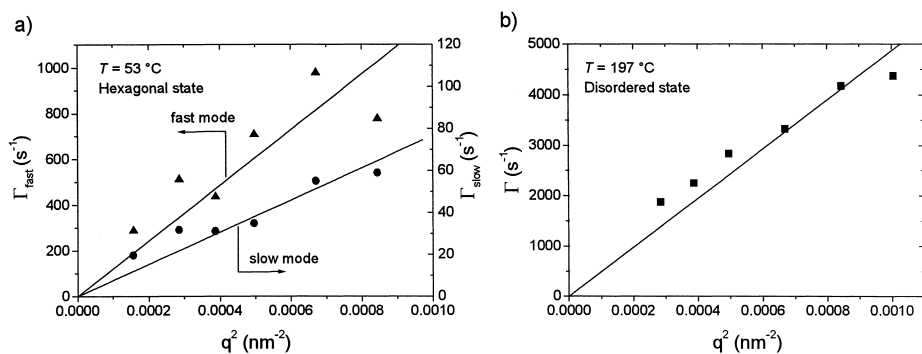


Fig. 4: Relaxation rates,  $\Gamma$ , of the modes observed in PEP-PDMS 21 vs.  $q^2$ .

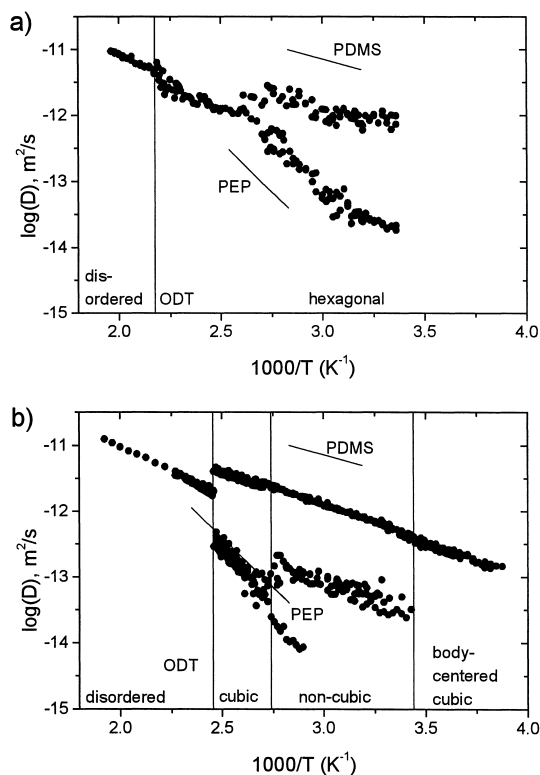


Fig. 5: Arrhenius-diagrams of the diffusion constants. The lines indicate the diffusion coefficients of pure PEP and PDMS homopolymer having the same molar mass as the PEP-PDMS diblock copolymers studied here.<sup>39-41)</sup> (a) PEP-PDMS 21, (b) PEP-PDMS 22.

together with their temperature dependence, which is related to the friction coefficient. The activation energy of PEP is 58 kJ/mol<sup>39,40)</sup> and the one of PDMS  $16 \pm 1$  kJ/mol,<sup>41)</sup> i.e. the friction coefficient of PEP is higher than that of PDMS. The activation energy of the single mode observed in the disordered state is  $30 \pm 2$  kJ/mol, the one of the slower mode in the ordered state is  $48 \pm 2$  kJ/mol (fitting range 24 – 112 °C), and the one of the fast mode is  $13 \pm 1$  kJ/mol (same fitting range). At the ODT, the extrapolated lines from disordered and the hexagonal state are offset by  $\Delta(\log D) = 0.1$ .

We assign the diffusive mode observed in the disordered state to the well-known heterogeneity mode. Its activation energy is only slightly higher than the volume average of PEP and PDMS (27 kJ/mol), and we attribute the discrepancy to concentration fluctuations which are expected to slow down the diffusion. At the ODT, the diffusion becomes discontinuously slower because of the formation of cylinders in a hexagonal lattice. Self-diffusion experiments by PFG NMR on the same sample showed that the diffusion in the hexagonal state is anisotropic with an anisotropy of  $D_{\text{par}}/D_{\text{perp}} \cong 5$  close to the ODT temperature to ~60 deep in the hexagonal state.<sup>24,28)</sup> This means a transition from three- to one-dimensional diffusion is encountered at the ODT. The activation energy of the slow mode is slightly lower than the one of PEP homopolymer. This mode may be due to (i) the diffusion of chains along the cylinders with the junctions remaining close to the cylinder interfaces and/or (ii) the diffusion of chains from cylinder to cylinder, i.e. across the PDMS matrix. Both processes should lead to fluctuations of the distance between the cylinders. For both processes, the friction is expected to be somewhat lower than the monomeric friction of PEP: In process (i), the major part of the chain is immersed in a PDMS matrix, and in process (ii), the chain leaves the PEP cylinder and joins the PDMS matrix where the monomeric friction is lower than in the PEP cylinder. However, the latter process is thermally activated because of the thermodynamic repulsion between the PEP block of the diffusing polymer and the PDMS matrix. The activation energy of the fast mode present below 127 °C is close to the one of PDMS homopolymer, i.e. the friction of PDMS dominates the dynamic process. We assign this mode to the heterogeneity mode of chains, which are not bound to cylinders ('free chains'), through the PDMS matrix. This also causes fluctuations of the cylinder distance. The amplitude of the fast mode increases as the ODT is approached from the hexagonal state, i.e. more and more chains are not bound to cylinders but diffuse through the matrix. Above ~127 °C the two modes cannot be resolved any longer, probably because the concentration profile

softens, making the diffusion coefficients of the free and the bound chains more and more similar.

### The Disordered and the Cubic Micellar Phase

From previously carried out measurements of the transmitted depolarized light intensity, three ordered phases have been identified in sample PEP-PDMS 22 (Fig. 1b). The middle phase ( $\sim 20 - 105^\circ\text{C}$ ) is weakly birefringent, i.e. non-cubic.<sup>25)</sup> Note that the signal in the non-cubic phase corresponds only to a few percent of the signal obtained in the hexagonal phase of sample PEP-PDMS 21. In SANS experiments on a shear oriented sample, we found that the low-temperature phase ( $T < \sim 20^\circ\text{C}$ ) is body-centered cubic (bcc). The middle, weakly birefringent phase ( $\sim 20 - 110^\circ\text{C}$ ) is non-cubic, but could not be identified on the basis of small-angle scattering experiments as no higher order Bragg reflections are present in the spectra.<sup>25)</sup> The high-temperature phase ( $\sim 110 - 134^\circ\text{C}$ ) is again cubic, but not necessarily body-centered cubic. Above  $T_{\text{ODT}} = 134^\circ\text{C}$ , the sample is disordered. Note that the OOT temperatures observed depend on the heating/cooling rates used. The values given here are from very slow experiments (10 h/data point, see Fig. 1b). The phase sequence observed in this sample is contradictory to what has been observed experimentally with other samples<sup>42-44)</sup> and with theoretical predictions.<sup>45-55)</sup>

Typical correlation functions measured in the VV geometry in the disordered and the three ordered phases are shown in Fig. 2b. Again, the (diffusive) cluster mode dominates the correlation curve in the disordered state: It contributes  $\sim 90\%$  of the total intensity. Using the Stokes-Einstein relationship together with the zero-shear viscosity, the cluster size is found to be  $\sim 130$  nm between the ODT temperature and up to  $250^\circ\text{C}$ .<sup>26)</sup> The relative amplitude of the cluster mode drops at the ODT temperature, and the slow mode (at  $\sim 0.1$ -10 s) becomes very broad (Fig. 2b). This slow mode thus shows similar characteristics to the one found in sample PEP-PDMS 21, and we do not analyze it further.

In order to analyze the remaining, faster modes, the correlation curves were analyzed by REPES, and above  $111^\circ\text{C}$ , the slowest mode was subtracted. The resulting distributions of relaxation times are shown in Fig. 3b. In the disordered state, a single mode is observed. In the cubic state right below the ODT temperature, two modes are observed, both modes having

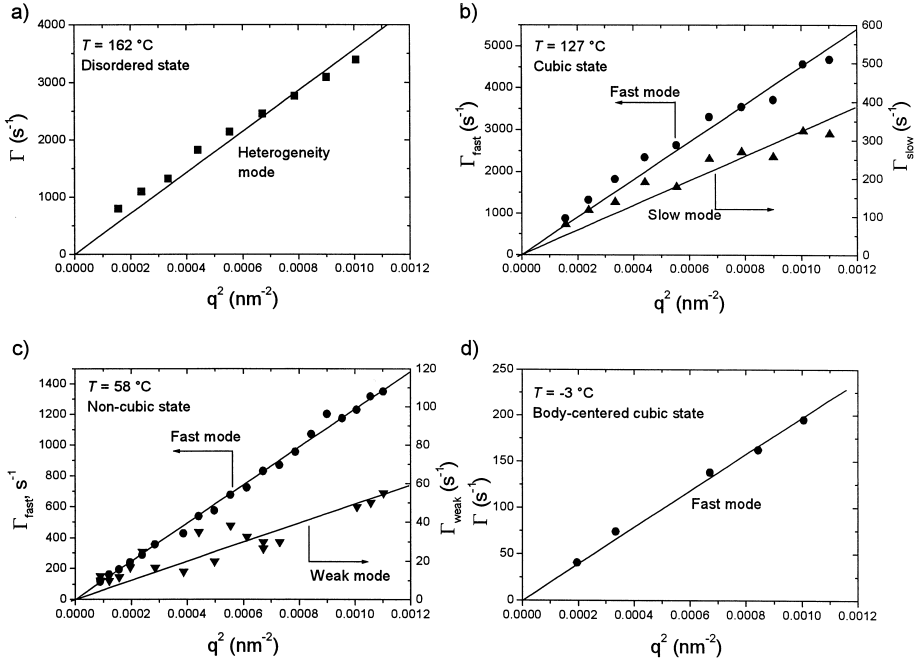


Fig. 6: Relaxation rates,  $\Gamma$ , of the modes observed in PEP-PDMS 22 vs.  $q^2$ .

approximately the same intensity. In the non-cubic phase, a weak mode appears in-between these two modes. Upon further cooling into the body-centered cubic phase, the weak mode disappears, and only one broad mode is present in the distribution function. The structural changes thus have a strong influence on the dynamics.

**The disordered state.** As with sample PEP-PDMS 21, one mode is present apart from the cluster mode (Fig. 3b). The peak in the distribution function becomes broader as the ODT temperature is approached, which we attribute to the onset of concentration fluctuations leading to PEP- and PDMS-rich environments. The relaxation rate of this mode is  $q^2$ -dependent (Fig. 6a), i.e. this mode is diffusive. The activation energy  $E_a$  for diffusion of the PEP-PDMS diblock copolymer is  $31.1 \pm 0.2$  kJ/mol. This value is slightly higher than the volume average of the activation energies of PDMS and PEP homopolymers (25 kJ/mol), which may be due to the formation of transient micelle-like domains. Such domains impose stronger hindrance to single-chain diffusion than the lamella- or cylinder-like fluctuations which may be formed in the symmetric sample<sup>10</sup> or in sample PEP-PDMS 21.

**High-temperature cubic phase.** In the cubic state right below the ODT temperature, the distribution functions display two peaks (Fig. 3b) apart from the cluster mode, which is not shown. For both modes,  $\Gamma \propto q^2$  (Fig. 6b). The diffusion constants of the fast mode are higher than in the disordered state. As seen from Figs. 3b and 5b, this mode is not sensitive to the OOT's, and its activation energy ( $\sim 20$  kJ/mol) is slightly higher than the one of pure PDMS. We conclude that this mode is related to the diffusion of free chains, i.e. the mutual diffusion of micelles relative to the free chains. The diffusion constant of this process is determined by the fastest diffusing species, i.e. the free chains. Such free chains in the bcc state have also been observed in an asymmetric poly(styrene-*block*-isoprene) sample.<sup>21,56)</sup> As expected, the diffusion of free chains depends only weakly on the actual structure of the PEP component (Fig. 5b). As the activation energy of PDMS is lower than the one of PEP homopolymer, the fast mode is faster than expected from extrapolating the heterogeneity mode from the disordered into the ordered state: The block copolymers can diffuse more rapidly through the PDMS matrix – where they encounter nearly exclusively PDMS segments – than in the disordered melt – where they encounter both PDMS and PEP segments. The slow mode is much slower than the heterogeneity mode in the disordered state. Its activation energy in this phase is  $66 \pm 3$  kJ/mol, thus close to the one of PEP homopolymer (Fig. 5b). Several processes can be discussed to be at the origin of this mode: (i) The mode could be due to the collective self-diffusion of a number of PEP micelles through the PDMS matrix. Note that the diffusion of single micelles through the lattice is unlikely because the block copolymer melt is a dense system without vacancies or interstitial sites like in atomic crystals, i.e. only collective rearrangements of a number of micelles are possible.<sup>27)</sup> The activation energy of this collective diffusion of PEP micelles through the PDMS matrix is determined both by the friction of PDMS and by the aggregation number of the micellar aggregate. As the aggregation number increases with decreasing temperature, the apparent diffusion constant decreases, which is indeed observed. (ii) Another process might be undulations of the lattice planes in the cubic lattice. Such undulations should give rise to a  $q^2$ -dependent mode,<sup>57)</sup> as is observed. We conclude that the slow mode must be due to collective dynamic processes of the block copolymer micelles, either the collective self-diffusion of micelles or undulations of the lattice planes.

**Intermediate non-cubic phase.** A third, weak, diffusive mode is present between the fast and the slow mode which persist from the cubic high-temperature phase (Figs. 3b, 5b, and 6c). The activation energy of this mode is  $19 \pm 1$  kJ/mol, thus similar to the one of PDMS homo-

polymer (Fig. 5b). From the non-vanishing transmitted depolarized light intensity and from the lack of higher-order reflections in SANS measurements, we concluded that the structure is non-cubic.<sup>25)</sup> The (degenerate) undulation mode observed in the cubic phase is thus expected to split up, i.e. we attribute the weak mode to undulations of the lattice planes along the third lattice direction.

**Low-temperature body-centered cubic phase.** In this phase the dynamics is very slow and the correlator time window only permits the analysis of the fast mode (Figs. 3b and 5b). It is still diffusive (Fig. 6d) and we thus again attribute it to the mutual diffusion of micelles and free chains.

## Summary and Conclusion

We have performed dynamic light scattering experiments on two asymmetric poly(ethylene-*alt*-propylene-*block*-dimethylsiloxane) (PEP-PDMS) diblock copolymer melts in order to study the effect of the morphology on the dynamics. One of the sample had a volume fraction of PEP of 0.25 and formed the disordered and the hexagonal state. The other sample had a PEP volume fraction of 0.22 and formed, besides the disordered state, a cubic, a non-cubic and the body-centered cubic structure as a function of temperature. In the disordered state, isotropic diffusion of single chains is observed with both samples. In the more asymmetric sample, a change of activation energy is observed in the disordered state, which we attribute to the onset of micelle-like concentration fluctuations. Deep in the hexagonal state, two diffusive modes are observed which we attribute to the self-diffusion of free chains through the PDMS matrix and to the self-diffusion of chains along and across the PEP cylinders. The diffusion of free chains is also observed in all ordered phases of the more asymmetric sample. In addition, slower modes are present, which we attribute to the collective diffusion of PEP micelles through the PDMS matrix or to undulations of lattice planes. The morphology thus has a strong influence on the molecular dynamics.

## Acknowledgements

P. Štěpánek gratefully acknowledges support by the Grant Agency of the Czech Republic (grant no. 203/99/0573). F. Rittig acknowledges support by the Deutsche Forschungsgemeinschaft (SFB 294). K. Almdal acknowledges support by the Danish Polymer Centre. We thank Dr. J.-U. Sommer, University of Freiburg, for fruitful discussions.

## References

1. E.g. L. Coppola, C. La Mesa, G.A. Ranieri, M. Terenzi, *J. Chem. Phys.* **98**, 5087 (1993).
2. A. G. Zilman, R. Granek, *Phys. Rev. Lett.* **77**, 4788 (1996)
3. F.S. Bates, G.H. Fredrickson, *Annu. Rev. Phys. Chem.* **41**, 525 (1990)
4. P. Štěpánek, T.P. Lodge, in: *Light Scattering. Principles and Development*, W. Brown (Ed.), Clarendon Press, Oxford 1996, and references therein
5. A.N. Semenov, G. Fytas, S.H. Anastasiadis, *Polymer Preprints (Am. Chem. Soc., Div. Polym. Chem.)* **35**, 618 (1994)
6. S.H. Anastasiadis, G. Fytas, S. Vogt, E.W. Fischer, *Phys. Rev. Lett.* **70**, 2415 (1993)
7. A.Z. Akcasu, M. Tombakoglu, *Macromolecules* **23**, 607 (1990)
8. R. Borsali, T.A. Vilgis, *J. Chem. Phys.* **93**, 3610 (1990)
9. P. Štěpánek, T.P. Lodge, *Macromolecules* **29**, 1244 (1996)
10. P. Štěpánek, K. Almdal, T.P. Lodge, *J. Polym. Sci., Polym. Phys. Ed.* **35**, 1643 (1997)
11. A. Hoffmann, T. Koch, B. Stühn, *Macromolecules* **26**, 7288 (1993)
12. T. Jian, A.N. Semenov, S.H. Anastasiadis, G. Fytas, F.-J. Yeh, B. Chu, S. Vogt, F. Wang, J.E.L. Roovers, *J. Chem. Phys.* **100**, 3286 (1994)
13. C.M. Papadakis, W. Brown, R.M. Johnsen, D. Posselt, K. Almdal, *J. Chem. Phys.* **104**, 1611 (1996)
14. T. Kanya, A. Patkowski, E. W. Fischer, J. Seils, H. Gläser, K. Kaji, *Acta Polymer.* **45**, 137 (1994)
15. M. Heckmeier, M. Mix, G. Strobl, *Macromolecules* **30**, 4454 (1997)
16. C.M. Dalvi, T.P. Lodge, *Macromolecules* **26**, 859 (1993)
17. G. Fleischer, F. Rittig, P. Štěpánek, K. Almdal, C.M. Papadakis, *Macromolecules* **32**, 1956 (1999)
18. S. Vogt, T. Jian, S.H. Anastasiadis, G. Fytas, E.W. Fischer, *Macromolecules* **26**, 3357 (1993)
19. M.W. Hamersky, M.A. Hillmyer, M. Tirrell, F.S. Bates, T.P. Lodge, E.D. von Meerwall, *Macromolecules* **31**, 5363 (1998)
20. A. Hoffmann, J.-U. Sommer, A. Blumen, *J. Chem. Phys.* **107**, 7559 (1997)
21. G. Fleischer, J. Kärger, B. Stühn, *Colloid & Polymer Science* **275**, 807 (1997)
22. T.P. Lodge, M.W. Hamersky, J.M. Milhaupt, R.M. Kannan, M.C. Dalvi, C.E. Eastman, *Macromol. Symp.* **121**, 219 (1997)
23. H. Yokoyama, E.J. Kramer, *Macromolecules* **31**, 7871 (1998)
24. F. Rittig, G. Fleischer, J. Kärger, C.M. Papadakis, K. Almdal, P. Štěpánek, *Macromolecules* **32**, 5872 (1999)
25. C.M. Papadakis, K. Almdal, K. Mortensen, M.E. Vigild, P. Štěpánek, *J. Chem. Phys.* **111**, 4319 (1999)
26. C.M. Papadakis, K. Almdal, K. Mortensen, F. Rittig, G. Fleischer, P. Štěpánek, *Eur. Phys. J. E* **1**, 275 (2000)
27. G. Fleischer, F. Rittig, J. Kärger, C.M. Papadakis, K. Mortensen, K. Almdal, P. Štěpánek, *J. Chem. Phys.* **111**, 2789 (1999)
28. F. Rittig, J. Kärger, C.M. Papadakis, G. Fleischer, P. Štěpánek, K. Almdal, *Phys. Chem. Chem. Phys.* **1**, 3923 (1999) and references therein
29. S. Ndoni, C.M. Papadakis, F.S. Bates, K. Almdal, *Rev. Sci. Instrum.* **66**, 1090 (1995)
30. M.E. Vigild, PhD thesis, University of Copenhagen, Oct 1997
31. K. Almdal, K. Mortensen, A.J. Ryan, F.S. Bates, *Macromolecules* **29**, 5940 (1996)
32. F.S. Bates, J.H. Rosedale, H.E. Bair, T.P. Russel, *Macromolecules* **22**, 2557 (1989)
33. J. Brandrup, E.H. Immergut, *Polymer Handbook*, 3<sup>rd</sup> ed., John Wiley & Sons, New York 1989
34. N. P. Balsara, B. A. Garetz, H. J. Dai, *Macromolecules* **25**, 6072 (1992)
35. J. Jakeš, *Czech J. Phys.* **B38**, 1305 (1988)

36. P. Štěpánek, R.M. Johnsen, *Collect. Czech. Chem. Commun.* **60**, 1941 (1995)
37. S.M. Chitanvis, *Phys. Rev. E* **57**, 1921 (1998)
38. E. W. Fischer, *Acta Polymerica* **201**, 183 (1993)
39. K.R. Shull, E.J. Kramer, F.S. Bates, J.H. Rosedale, *Macromolecules* **24**, 1383 (1991)
40. D. Pearson, L.J. Fetters, W.W. Graessley, G. Ver Strate, E. von Meerwall, *Macromolecules* **27**, 711 (1994)
41. M. Appel, G. Fleischer, *Macromolecules* **26**, 5520 (1993)
42. K. Almdal, K.A. Koppi, F.S. Bates, *Macromolecules* **26**, 4058 (1993)
43. K.A. Koppi, M. Tirrell, F.S. Bates, K. Almdal, K. Mortensen, *J. Rheol.* **38**, 999 (1994)
44. N. Sakamoto, T. Hashimoto, C.D. Han, D. Kim, N.Y. Vaidya, *Macromolecules* **30**, 1621 (1997)
45. L. Leibler, *Macromolecules* **13**, 1602 (1980)
46. G.H. Fredrickson, E. Helfand, *J. Chem. Phys.* **87**, 697 (1987)
47. E. Helfand, Z.R. Wasserman, in: *Developments in Block Copolymers-I*, I. Goodman (Ed.), Applied Science Publishers, London 1982
48. T. Ohta, K. Kawasaki, *Macromolecules* **19**, 2621 (1986)
49. J.D. Vavasour, M.D. Whitmore, *Macromolecules* **25**, 5477 (1992)
50. A.N. Semenov, *Macromolecules* **22**, 2849 (1989)
51. I.W. Hamley, F.S. Bates, *J. Chem. Phys.* **100**, 6813 (1994)
52. M.W. Matsen, F.S. Bates, *Macromolecules* **29**, 1091 (1996)
53. A.-C. Shi, J. Noolandi, R.C. Desai, *Macromolecules* **29**, 6487 (1996)
54. M. Laradji, A.-C. Shi, J. Noolandi, R.C. Desai, *Macromolecules* **30**, 3242 (1997)
55. S. Qi, Z.-G. Wang, *Phys. Rev. E* **55**, 1682 (1997)
56. M. Schwab, B. Stühn, *Phys. Rev. Lett.* **76**, 924 (1996).
57. P.G. de Gennes, *The physics of liquid crystals*, Ch. 7, Clarendon Press, Oxford 1974